Atypical small GTPase RABL3 interacts with RAB11 to regulate early ciliogenesis in human cells

Running title: RABL3 in ciliary vesicle formation

[1, 2, 3]Tetsuo Kobayashi, [1,3]Tatsuya Ikeda, [1]Reo Ota, [1]Takafumi Yasukawa, and [1]Hiroshi Itoh

[1]Division of Biological Science, Graduate School of Science and Technology, Nara Institute of Science and Technology, 8916-5 Takayama, Ikoma, Nara 630-0192, Japan

[2]Corresponding author: kobayt@bs.naist.jp

[3]These authors contributed equally to this work

Key words: primary cilia, RABL3, RAB11, ciliary vesicle

Abstract

Primary cilia are near-ubiquitously assembled on cells in the human body and are broadly associated with genetic diseases and cancers. In the early stage of ciliogenesis, the ciliary vesicle (CV) is formed on the mother centriole, which nucleates the primary cilium. However, the regulatory mechanisms underlying CV formation have not yet been fully elucidated. Here, we found that the atypical small GTPase RAB-Like 3 (RABL3) is necessary to assemble primary cilia in human cells. RABL3 directly interacts with RAB11, which is involved in CV formation. RABL3 localizes around the centrosome during early ciliogenesis, reminiscent of RAB11 dynamics. Furthermore, RABL3 positively controls the CV formation like RAB11. These findings suggest that RABL3 plays an important role, in cooperation with RAB11, in CV formation during early ciliogenesis.

Introduction

The centrosome contains two cylinder-like structures, termed mother and daughter centrioles. The mother centriole is equipped with distal and subdistal appendages (DA and SDA, respectively) that are absent from the daughter centriole. Centrioles nucleate spindles during mitosis, whereas the mother centriole becomes the base of a sensory organelle called the primary cilium during interphase (Kobayashi and Dynlacht, 2011; Sánchez and Dynlacht, 2016). The primary cilium protrudes from the cell surface of most mammalian cells and contains multiple signaling molecules (Ishikawa and Marshall, 2011). Structural and functional anomalies in primary cilia are implicated in a broad spectrum of genetic diseases and cancers (Eguether and Hahne, 2018; Liu et al., 2018; Reiter and Leroux, 2017). In cultured mammalian cells, serum deprivation from the culture medium induces a transition from the mother centriole to the primary cilium.

A small vesicle, termed ciliary vesicle (CV), covers the top of the mother centriole in the early stage of the intracellular ciliogenesis in human cells (SOROKIN, 1962). Pre-ciliary vesicles (PCVs), which are thought to be derived from the Golgi, are initially attached to the DA of the mother centriole, where they are referred to as distal appendage vesicles (DAVs), and DAVs assemble into the CV (Shakya and Westlake, 2021). The CV extends along with microtubule elongation and finally develops into the ciliary membrane (CM), encapsulating the ciliary axoneme. Thus far, mounting studies have indicated that several proteins regulate CM formation processes in a stepwise manner, including the RAB-family small GTPases. Myo-Va occupies the PCV and aids in the trafficking of PCVs to the DA (Wu et al., 2018). EHD1/3, SNAP29, PACSIN1/2,

and MICAL-L1 mediate CV assembly from DAVs (Insinna et al., 2019; Lu et al., 2015). The small GTPase RAB34 is also required for CV assembly step (Ganga et al., 2021; Stuck et al., 2021). The small GTPase RAB8 appears to be involved in the extension of CV to develop CM (Lu et al., 2015). Two ciliopathy-related proteins, Talpid3 and CEP290, are necessary for RAB8 recruitment and proper CV development (Kobayashi et al., 2014). RAB8 is activated by a guanine nucleotide exchange factor (GEF), Rabin8, and the small GTPase RAB11 (Knödler et al., 2010). RAB11 regulates GEF activity and centrosome targeting of Rabin8 (Knödler et al., 2010; Westlake et al., 2011). Recently, it was shown that lysophosphatidic acid (LPA)/LPA Receptor-1-dependent PI3K/Akt signaling controls RAB11 activation during ciliogenesis (Walia et al., 2019).

RAB-Like 3 (RABL3) is a member of the RABL family, comprising a RAB GTPases subfamily (Colicelli, 2004). RABL proteins are devoid of sites for lipid modification and some conserved residues in GTP-binding proteins (Blacque et al., 2018; Homma et al., 2021). RABL3 is upregulated in several cancers and is required for their proliferation and migration (An et al., 2017; Ge et al., 2019; Li et al., 2010; Ma et al., 2021; Pan et al., 2017; Usman et al., 2020; Xu et al., 2021; Zhang et al., 2016). Mutations in *rabl3* are correlated with heritable pancreatic cancer (Nissim et al., 2019). A recent study showed that RABL3 is crucial for lymphoid function, and that its knockout mice are embryonic lethal (Zhong et al., 2020). Interestingly, four of the six RABL proteins are known to be involved in molecular trafficking to and within primary cilia. RABL4/IFT27 and RABL5/IFT22 comprise the intraflagellar transport (IFT) machinery, a universally conserved protein complex that bi-directionally conveys

78 molecules in primary cilia (Nakayama and Katoh, 2018). RABL2 controls anterograde
79 IFT and trafficking of ciliary G-protein-coupled receptors (Dateyama et al., 2019; Kanie
80 et al., 2017; Nishijima et al., 2017). A recent study showed that RABL2 ensures export
81 of ciliary proteins (Duan et al., 2021). A proteomic analysis using mouse photoreceptor
82 sensory cilia suggested RABL3 as a cilia-related protein (Liu et al., 2007); however, it
83 is unknown whether and how RABL3 is associated with primary cilia.
84 In this study, we investigated normal diploid human cells depleted of RABL3 and
85 discovered that RABL3 is required to assemble primary cilia. A proteomic approach
86 identified RAB11 as a RABL3-binding protein. RABL3 directly interacts with and is
87 stabilized by RAB11 *in vitro*. RABL3 accumulated around the centrosome during early
88 ciliogenesis, similar to RAB11. Furthermore, RABL3 depletion impaired CV formation,
89 but ectopic RABL3 expression promoted CV formation, phenocopying ablation and
90 overexpression of RAB11, respectively. Altogether, these results suggest that RABL3
91 cooperates with RAB11 and regulates the CV formation during early ciliogenesis in
92 human cells.
93

Results

RABL3 is required for primary ciliogenesis in RPE1 cells

To investigate the consequences of RABL3 depletion in normal diploid human cells, we generated RABL3-mutated retinal pigment epithelial (RPE1) cells by CRISPR/Cas9-mediated gene editing. Sequence analysis indicated heterozygous mutations in two clones, Rabl3-1 and Rabl3-2 (Figure S1A). While a four-nucleotide deletion in one allele led to a premature stop codon before the G4 domain in Rabl3-1, a three-nucleotide in-frame deletion resulting in replacement of two amino-acids, (glutamine and asparagine) with one amino-acid (histidine) occurred in another allele. This QN motif is conserved in vertebrate RABL3 (Figure S1B), suggesting that this mutation seriously impairs RABL3. In contrast, mutations in both alleles lead to premature stop codons in Rabl3-2. We found a substantial decrease in RABL3 protein levels in both clones by immunoblotting analysis, although RABL3 was faintly detected in Rabl3-1 as predicted by sequence analysis (Figure 1A).

We then investigated primary cilia formation in RABL3-mutated cells. Primary cilia were visualized by immunofluorescence experiments with two specific antibodies against glutamylated tubulin (Glu. Tub.) and ARL13B. The wild-type (WT) RPE1 cells assembled primary cilia when induced to quiescence by depriving the serum in the culture medium (Figure 1B, C). In contrast, Rabl3-1 and Rabl3-2 cells formed significantly fewer primary cilia than WT cells (Figure 1B, C). We next conducted rescue experiments to verify that the de-ciliation phenotype in RABL3-mutated cells was due to the loss of RABL3. Ectopic expression of RABL3 significantly restored

116 primary cilia in Rabl3-1 and Rabl3-2 cells (Figure 1D, E). In contrast, the
117 RABL3/S20N mutant, which is expected to fail to bind GTP, namely a negatively
118 locked mutant, did not ameliorate the phenotype (Figure 1D, E). These results suggest
119 that RABL3 with GTP-binding capacity is required for ciliogenesis. We also performed
120 siRNA-mediated knockdown experiments. The protein expression of endogenous
121 RABL3 was considerably decreased by introducing two individual siRNAs targeting
122 RABL3 (Figure 1F). We observed a significant reduction in primary cilia assembly in
123 these RABL3-ablated RPE1 cells (Figure 1G). Collectively, these results strongly
124 suggest that RABL3 is a requisite for primary cilia formation in RPE1 cells.

125 **RABL3 interacts with and is stabilized by RAB11**

126 To uncover the mechanistic role of RABL3 in primary ciliogenesis, we performed a
127 proteomic screen to identify RABL3-interacting proteins. Immunoaffinity
128 chromatography and subsequent mass spectrometric analysis identified a peptide
129 common to two close paralogs of small GTPases, RAB11A and RAB11B, in RABL3
130 immunoprecipitation (Figure S2A, B). We co-expressed Flag-tagged RABL3 and
131 GFP-fused RAB11A in HEK293T cells and performed anti-Flag immunoprecipitation
132 to test if they interact in cells and found that RABL3 co-precipitated with RAB11A
133 (Figure 2A). We subsequently performed similar experiments using cells co-expressing
134 RABL3/WT or S20N, and RAB11A/WT, actively locked Q70L mutant, or negatively
135 locked S25N mutant, and found efficient co-precipitation of RABL3/S20N and
136 RAB11A/Q70L (Figure 2A). Reciprocal immunoprecipitation using an anti-GFP
137 antibody confirmed similar binding properties (Figure 2B). These results suggest that

the negative form of RABL3 preferentially interacts with the active form of RAB11A.

We next investigated the direct interaction between RABL3 and RAB11. To this end, we purified recombinant RABL3 and RAB11A proteins from bacterial lysates (Figure 2C). We then performed a pull-down assay using glutathione sepharose with buffer containing Mg^{2+}, and found that GST-RAB11A specifically pulled down RABL3 (Figure 2D, left), demonstrating their direct binding. In contrast, adding a non-hydrolyzable GTP analog GTPγS or GDP substantially abrogated their association (Figure 2C, middle and right). This result shows that RABL3 and RAB11 fail to bind to each other in the same guanine nucleotide forms, consistent with previous immunoprecipitation assays that the negative form of RABL3 associated with the active form of RAB11A.

A previous study showed that RABL4/IFT27 binds to the small GTPase ARL6 and prevents the aggregation of ARL6 *in vitro* (Liew et al., 2014). Because of the analogous RABL-small GTPase interaction, we performed a similar turbidity assay using the recombinant RABL3 and RAB11A proteins to test mutual chaperone activity. The optical density at 350 nm was monitored to detect the insoluble (precipitated) proteins (Liew et al., 2014). While RABL3 was precipitated by incubation at 37 °C for 12 min, the precipitation was significantly reduced in the mixture of RABL3 and GST-RAB11A (Figure 2E). In contrast, GST-RAB11A was soluble in this assay. These results suggest that RAB11 stabilizes RABL3 *in vitro*.

RABL3 accumulates around the centrosome during early ciliogenesis

We assessed the subcellular localization of RABL3 in RPE1 cells by performing

160 immunofluorescence assays. Multiple puncta were detected throughout the cells with a
161 RABL3 antibody (Figure 3A, upper left), and these puncta were almost completely
162 absent in Rabl3-2 cells (Figure 3A, lower left), indicating that the RABL3 antibody
163 specifically recognizes endogenous RABL3 in RPE1 cells. Endogenous RABL3
164 incrementally accumulated in the vicinity of the centrosome during induction to
165 quiescence for 6 h in RPE1 cells but not in Rabl3-2 cells (Figure 3A, right, 3B). These
166 RABL3-positive puncta around CEP164-positive mother centriole partially overlapped
167 with RAB11, which is known to accumulate around the centrosome during early
168 ciliogenesis (Figure 3C) (Westlake et al., 2011). In addition, a fraction of RABL3
169 co-localized with RAB11 and GM130, a canonical marker of the Golgi, after 6 h of
170 serum-starvation (Figure 3D). These results collectively indicate that RABL3 is partly
171 located around the centrosome and the Golgi apparatus and co-localizes with RAB11
172 during early ciliogenesis. Furthermore, to evaluate guanine nucleotide-form-dependent
173 localization of RABL3 during ciliogenesis, RPE1 cells expressing Myc-tagged
174 RABL3/WT or S20N were cultured in the serum-starved medium for 6 h. Although
175 RABL3/WT was distributed uniformly or marginally around the centrosome,
176 RABL3/S20N was clearly concentrated at the centrosome (Figure 3E, right). These
177 observations suggest that the negative form of RABL3 is recruited to the centrosome
178 during early ciliogenesis.

179 **RABL3 depletion impedes early ciliogenesis**

180 We attempted to reveal the role of RABL3 in the primary cilium formation process.
181 We first examined CP110, which localizes to both mother and daughter centrioles in

cycling cells and disappears from the mother centriole during early ciliogenesis (Spektor et al., 2007). We found that cells with two CP110 dots were significantly increased upon silencing RABL3 (Figure 4A, B), suggesting that it is required for the CP110 removal from the mother centriole. RAB11 depletion also hampered primary ciliogenesis and the loss of CP110 dots (Figure 1F, G, 4A, B). Next, we explored GFP-Rabin8 vesicles that accumulate around the centrosome immediately after serum withdrawal in RPE1 cells (Westlake et al., 2011). Ablation of RABL3 suppressed the accumulation of GFP-Rabin8 around the centrosome (Figure 4C, D). RAB11 knockdown induced a similar phenotype (Figure 4C, D), consistent with previous reports (Lu et al., 2015; Westlake et al., 2011). These results suggest that RABL3 is a prerequisite for the early steps of primary cilia formation, similar to RAB11.

RABL3 positively controls CV formation

As GFP-Rabin8 vesicles are thought to provide membrane components to assemble ciliary membrane structures (CV and CM) (Shakya and Westlake, 2021), we established GFP-Smoothened (SMO)-expressing RPE1 cells to visualize their formation (Lu et al., 2015). While elongated GFP-SMO along with the axoneme, indicating CM, was observed in control cells, RABL3 or RAB11 depletion abolished GFP-SMO-positive foci at the centriole (Figure 5A, B), suggesting that RABL3 and RAB11 are required for GFP-SMO-positive CV (SMO^+ CV) formation. In contrast to RABL3 and RAB11, silencing of RAB8 allowed SMO^+ CV formation irrespective of suppressed ciliation (Figure 1F, G, 5A, B). These data suggest that RABL3 and RAB11 play overlapping roles in CV formation, whereas RAB8 is necessary after CV formation, as described

204 previously (Lu et al., 2015).

205 We further examined CV formation by using an anti-Myo-Va antibody, which is
206 known to mark both initial CV without GFP-SMO (Myo-Va^{+}/GFP-SMO^{-} CV) and
207 subsequent CV (Myo-Va^{+}/GFP-SMO^{+} CV) (Wu et al., 2018). As expected, single
208 Myo-Va-positive dots were detected adjacent to the centriole, and some of them grossly
209 overlapped with GFP-SMO-dots when RPE1 cells were induced to quiescence for 6 h
210 (Figure 5C, S3). The number of Myo-Va^{+} CV was significantly lower in
211 RABL3-mutated cells than that in WT cells at 6 h of starvation, whereas it was
212 equivalently observed in both cells after 3 h of starvation (Figure 5D). These results
213 suggest that RABL3 is dispensable for initial Myo-Va^{+}/GFP-SMO^{-} CV formation but is
214 required for later Myo-Va^{+}/GFP-SMO^{+} CV formation (Figure S4). A similar phenotype
215 was also induced by the silencing of RAB11 (Figure 5E). Conversely, ectopic
216 expression of WT or active mutants, but not negative mutants of RABL3 or RAB11A,
217 enhanced Myo-Va^{+} CV formation (Figure 5F). Moreover, increased Myo-Va^{+} CV by
218 overexpression of RAB11A/QL was partly but significantly inhibited in
219 RABL3-mutated cells (Figure 5G). Collectively, these results suggest that the
220 RAB11-RABL3 axis positively controls CV formation during ciliogenesis in human
221 cells.
222
223
224

Discussion

Of six RABL proteins, five (2A, 2B, 3, 4, and 5) are similar to typical small GTPases in size (185–266 aa in humans), in contrast RABL6 (730 aa in humans) is a relatively large protein. Based on our findings, it is possible to suggest that all small GTPase-type RABL proteins play cilia-related functions in human cells. While other small RABL proteins localize to the basal body and/or the ciliary axoneme, RABL3 shows a wider distribution throughout cells. Since RABL3 has been shown to pertain to multiple cellular events, including KRAS signaling, lymphopoiesis, and cancer cells proliferation and migration (An et al., 2017; Ge et al., 2019; Li et al., 2010; Ma et al., 2021; Nissim et al., 2019; Pan et al., 2017; Usman et al., 2020; Xu et al., 2021; Zhang et al., 2016; Zhong et al., 2020), RABL3 may be located broadly to play distinct roles depending on target molecules, interacting proteins, and/or cell types.

The RABL3-RAB11 interaction that we have demonstrated in this study is analogous to other RABL-small GTPase associations in that RABL4/IFT27 and RABL5/IFT22 bind to the small GTPase ARL6/BBS3, and these interactions occur during ciliary events. GTP-bound RABL4 associates with nucleotide-free or GDP-bound ARL6 in human cells (Liew et al., 2014). Both RABL4 and RABL5 stabilize ARL6 (Liew et al., 2014; Xue et al., 2020). Interestingly, RABL4 has been reported to be structurally akin to RAB11 (Bhogaraju et al., 2011). Therefore, our findings and previous reports indicate that similar GTP-bound small GTPases (RAB11 and RABL4) stabilize GDP-bound or nucleotide-free small GTPases (RABL3 and ARL6, respectively), both of which are related to ciliary functions in human cells. However, immunoblotting and

247 immunostaining for RABL3 in RAB11-depleted cells did not detect a decrease in
248 RABL3 expression (Figure 1F, data not shown). This is likely because RAB11 stabilizes
249 RABL3 in a specific location and/or time-point during ciliogenesis. Our
250 immunoprecipitation and subcellular localization analyses suggest that the chaperone
251 effect of RAB11 could contribute to the recruitment of GDP-bound or nucleotide-free
252 RABL3 to the centrosome. As RABL3/WT but not RABL3/S20N rescued de-ciliation
253 in RABL3-mutated cells, GTP-binding is required for RABL3 function during
254 ciliogenesis. Therefore, we hypothesize that GDP on RABL3 is probably replaced with
255 GTP by GEF(s) around the centrosome, and then the GTP-bound RABL3 promotes CV
256 formation through effector protein(s). Future work should identify the GEF(s) and
257 effector(s) of RABL3 during ciliogenesis.
258 Presenting study may have uncovered a previously unidentified step in the CV
259 formation pathway in human cells. RABL3 is dispensable for initial CV formation but
260 is required for the following step, denoted “CV maturation” (Figure S4). Once the initial
261 CV is assembled form DAVs, RABL3 is required for the subsequent “CV maturation”
262 step in which several ciliary membrane proteins such as GFP-SMO are probably loaded
263 to the CV. RAB11 is also involved in CV maturation through its association with
264 RABL3. This hypothesis agrees with a previous study in which initial Myo-Va^{+} CV
265 formation was unaffected by depletion or overexpression of RAB11 (Wu et al., 2018).
266 After CV maturation, RAB8 promotes the CV extension, which is also activated by
267 RAB11 via Rabin8 (Lu et al., 2015). In the present model, RAB11 in the GTP-bound
268 state controls continuous CM formation processes through its association with RABL3

269 or Rabin8-RAB8. A recent study showed that serum deprivation triggers primary cilia
270 formation through PI3K/Akt and downstream RAB11 (Walia et al., 2019). Therefore, it
271 is feasible that RAB11 regulates multiple steps in early ciliogenesis, including
272 RABL3-dependent CV maturation. It will be of interest to investigate whether serum
273 deprivation and/or the PI3K/Akt axis impact the RABL3-dependent CV maturation step.
274 Furthermore, as RABL3-mutated zebrafish exhibited developmental phenotypes
275 reminiscent of cilia-loss mutants (Nissim et al., 2019), future genetic studies may lead
276 to the identification of unknown mutations in *Rabl3*, which cause cilia-related diseases.
277

Materials & Methods

Cell culture

HEK293T cells (from B. D. Dynlacht) were grown in DMEM (Nacalai tesque) supplemented with 10% Calf Serum (Thermo Fisher Scientific) and 100 units/ml penicillin and 100 μg/ml streptomycin (P/S) (Nacalai tesque). hTert-RPE1 (RPE1) (from B. D. Dynlacht), GFP-SMO-RPE1 (generated in this study), and GFP-Rabin8-RPE1 (from P. K. Jackson) were grown in DMEM supplemented with 10% Fetal Bovine Serum (FBS) (Biosera) and P/S.

Antibodies

Antibodies used in this study include rabbit anti-RABL3 (1:500 (IF), 1:1000 (WB), Abcam, ab196024), mouse anti-glutamylated tubulin (GT335) (1:1000 (IF), Adipogen, AG-20B-0020), rabbit anti-ARL13B (1:1000 (IF), Proteintech, 17711-1-AP), rabbit anti-GM130 (1:1000 (IF), BD biosciences, #610822), mouse anti-RAB11 (1:100 (IF), 1:1000 (WB), Millipore, 05-853), rabbit anti-RAB8A (1:1000 (WB), Proteintech, 55296-1-AP), mouse anti-Centrin (1:1000 (IF), Millipore, 04-1624), rabbit anti-CP110 (1:1000 (IF), from B. D. Dynlacht) (Chen et al., 2002b), goat anti-CEP164 (1:200 (IF), Santa Cruz, sc-240226), rabbit anti-Myosin-Va (1:500 (IF), Novus, NBP1-92156), mouse anti-β-Actin (1:1000 (WB), Santa Cruz, sc-47778), rabbit anti-FLAG (1:1000 (WB), Sigma Aldrich, F7425), rabbit anti-Myc (1:1000 (WB), MBL, #562), rabbit anti-GST (1:1000 (WB), MBL, PM013), and rabbit anti-GFP (1:1000 (WB), Santa Cruz, sc-9996).

Plasmids

To generate Flag-RABL3 or Myc-RABL3, human RABL3 fragment encoding residue 1-236 was amplified by PCR using forward primer 5'-AAGAATTCATGGCGTCCCTGGATCGGGT-3' and reverse primer 5'-AAGTCGACTCAGTCATAATGAAGGCTCTT-3', and sub-cloned into pCMV5-Flag or pCMV5-Myc (from K. Kontani and T. Katada). RABL3/S20N plasmid was made by PCR-based mutagenesis using forward primer 5'-AATTCGTTAGTCCATCTCCT-3' and reverse primer 5'-TTTCCCAACACCTGAGTCTC-3'. pEGFP-C2-hRAB11A was obtained from K. Kontani and T. Katada. RAB11A/S25N and Q70L constructs were made by PCR-based mutagenesis using forward primer 5'-AATAATCTCCTGTCTCGATTTAC-3' and reverse primer 5'-CTTTCCAACACCAGAATCTC-3', and forward primer 5'-CTAGAGCGATATCGAGCTAT-3' and reverse primer 5'-CCCTGCTGTGTCCCATATCT-3', respectively. To generate Myc-RAB11A, RAB11A/S25N, or RAB11A/Q70L, hRAB11A fragments were sub-cloned into pCMV5-Myc. To generate recombinant GST-RABL3 and GST-RAB11A, hRABL3 and hRAB11A fragments were sub-cloned into pGEX6P1. To make PX459-hRABL3, annealed oligo (5'-CACCGATGACCAACGACGCAAGTTT-3' and 5'-AAACAAACTTGCGTCGTTGGTCATC-3') was inserted into PX459 (pSpCas9(BB)-2A-PuroV2.0) (Addgene) (Ran et al., 2013). The plasmid expressing Flag-RABL2B was previously described (Dateyama et al., 2019). pGEX6P1-GFP nanobody was obtained from Y. Katoh and K. Nakayama (Katoh et al., 2015). pEGFP-mSmo was obtained from Addgene (Chen et al., 2002a).

Plasmid transfection into HEK293T cells was performed using PEI Max (Polysciences) according to the manufacturer's instruction. Plasmid transfection into RPE1 cells was performed using ViaFect (Promega) according to the manufacturer's instruction.

RNAi

siRNA oligos used in this study were siRABL3#1 (Ambion, s49874), siRABL3#2 (Ambion, s57630), siRAB8A (5'-GACAAGUUUCCAAGGAACGtt-3', Sigma Aldrich), siRAB8B (5'-GACAAGUGUCAAAAGAAAGtt-3', Sigma Aldrich), siRAB11A (5'-UGUCAGACAGACGCGAAAAtt-3', Sigma Aldrich), siRAB11B (5'-GCACCUGACCUAUGAGAACtt-3', Sigma Aldrich). The siRNA for luciferase (siLuc) was described previously (Kobayashi et al., 2017). For RNAi, 2 x 10^4 RPE1 cells were seeded in 24-well plate and cultured for 24 hrs. After transfection of 20 pmol siRNA using Lipofectamine RNAiMAX (Invitrogen), cells were cultured in normal medium for 24 hrs and subsequently incubated in serum starved medium.

Immunoprecipitation and Western blotting

Cells were lysed with lysis buffer (50 mM Hepes-NaOH pH 7.5, 150 mM NaCl, 5 mM $MgCl_2$, 0.5% NP-40, 1 mM DTT, 0.5 mM PMSF, 2 μg/ml leupeptin, and 10% Glycerol) at 4 °C for 30 minutes. For immunoprecipitation, 1 mg of the resulting supernatant after centrifugation was incubated with anti-Flag agarose beads (Sigma Aldrich) or GFP-nanobody at 4 °C for 2 hrs. The resin was washed with lysis buffer, and the bound polypeptides were analyzed by SDS-PAGE and immunoblotting. 10 μg of lysate was loaded in the input (IN) lane.

Immunofluorescence microscopy

Immunofluorescence microscopy was performed as described previously (Kobayashi et al., 2017). Quantification analysis of fluorescence was performed using ImageJ (Kobayashi et al., 2020).

Generation of RABL3-mutated RPE1 cells

PX459-hRABL3 plasmid was transfected into RPE1 cells using Lipofectamine 2000 (Invitrogen). After 24 hrs, cells were cultured in medium with 10 μg/ml puromycin (Nacalai tesque) for 3 days and singly plated into 96-well plates. Genome DNA was extracted from survival cells using QuickExtract DNA Solution 1.0 (epicentre), and mutations were determined by sequencing against amplified PCR products including guide RNA target sequence. Primers for PCR amplification and sequencing are listed in Table S1.

Generation of GFP-SMO-RPE1 cells

To generate GFP-SMO-expressed cells, RPE1 cells were transfected with pEGFP-mSMO plasmid and subsequently cultured in medium with 1 mg/ml G418 (Nacalai tesque) for 12 days. Isolated colonies were examined by immunofluorescence.

Recombinant proteins

E. coli BL21(DE3) pLysS cells (TOYOBO) harboring pGEX6P1, pGEX6P1-RABL3 or pGEX6P1-RAB11A were cultured in LB/2% Glucose medium at 37 °C until OD_{600} = 0.3. After 0.2 mM isopropyl β-D-1-thiogalactopyranoside (IPTG, Nacalai tesque) treatment, cells were subsequently incubated at 37 °C for 2 hrs. Collected cells by centrifugation were suspended with extraction buffer (50 mM Tris-HCl (pH 8.0), 100 mM NaCl, 5 mM $MgCl_2$, 1 mM DTT, 10% Glycerol, 0.5 mM PMSF, 2 μg/ml leupeptin),

and solubilized with Triton-X 100 with final concentration of 0.5% after sonication. The supernatant after centrifugation at 17,000 g at 4 °C for 1 hr was incubated with Glutathione Sepharose 4B (GE healthcare) at 4 °C for 3 hrs. After washing with Wash Buffer (50 mM Tris-HCl (pH 8.0), 100 mM NaCl, 5 mM $MgCl_2$, 1 mM DTT, 10% Glycerol, 0.5% Triton-X100), the resin was incubated with Wash Buffer containing 15 mM Glutathione (Nacalai tesque) at 4 °C for 20 min to obtain GST or GST-RABL3. The resin after washing was incubated with Wash Buffer containing PreScission Protease (GE healthcare) to elute RAB11A by cleavage at 4 °C for 16 hrs. The eluate containing recombinant proteins was passed through a PD-10 column (GE healthcare) to exchange buffer with Store Buffer (50 mM Tris-HCl (pH 7.5), 100 mM NaCl, 1 mM $MgCl_2$, 1 mM DTT, 10% Glycerol, 0.1% Triton-X100). For Turbidity assay, proteins were solubilized in Store Buffer-2 (50 mM Tris-HCl (pH 7.5), 100 mM NaCl, 1 mM $MgCl_2$, 1 mM DTT).

GFP-nanobody

E. coli BL21(DE3) pLysS cells harboring pGEX6P1-GFP nanobody were cultured in LB/2% Glucose medium at 37 °C until OD_{600} = 0.5. After 0.1 mM IPTG treatment, cells were subsequently incubated at 20 °C for 20 hrs. Collected cells by centrifugation were lysed and purified using Glutathione-Sepharose 4B as described previously (Katoh et al., 2015).

***In vitro* binding assay**

0.5 μM RABL3 and 0.05 μM GST or GST-RAB11 were mixed with Glutathione-Sepharose 4B in the presence of 10 μM GTPγS (Sigma Aldrich) or 10 μM

GDP (Sigma Aldrich) in Store Buffer. The mixture was incubated at 25 °C for 1 hr, and then rotated at 4 °C for 2 hrs. The resin was washed with Store Buffer, and the bound polypeptides were analyzed by SDS-PAGE and immunoblotting.

Turbidity assay

20 μM RABL3 and 20 μM GST or GST-RAB11 were mixed on ice in Store Buffer-2. The mixture was incubated at 37 °C, and optical density (OD) was measured at 350 nm using Nanodrop 2000c (Thermo Scientific) every 3 mins.

Identification of RABL3-interacting proteins

The procedures were basically performed as described previously (Kobayashi et al., 2011). Briefly, Flag-RABL3 or Flag-RABL2B was expressed in HEK293T cells and immunoprecipitated with anti-Flag agarose beads at 4 °C for 3 hrs. Bound proteins were eluted with Flag peptide (Sigma Aldrich) for 30 min, and the resultant eluates were TCA precipitated and analyzed by SDS-PAGE. After Coomassie staining, the gel was subjected to mass spectrometric analysis performed at NAIST mass spectrometric laboratory.

Statistical Analysis

The statistical significance of the difference was determined using two-tailed Student's *t*-test (except for Fig. 5B) or *x*-squared test (Fig. 5B). Differences were considered significant when $p < 0.05$. **, $p < 0.01$; *, $p < 0.05$, ##, $p < 0.01$; #, $p < 0.05$.

408 **Acknowledgements**

409 We thank B. D. Dynlacht (New York University) for an anti-CP110 antibody, hTert

410 RPE1, and HEK293T cells; P. K. Jackson (Stanford University) for GFP-Rabin8-RPE1

411 cells; Y. Katoh and K. Nakayama (Kyoto University) for pGEX6P1-GFP nanobody; T.

412 Katada and K. Kontani (University of Tokyo) for pCMV5-Flag, pCMV5-Myc, and

413 pEGFP-C2-hRAB11A. We thank Y. Fukao and R. Kurata (NAIST) for mass

414 spectrometric analysis.

415 T. K. was supported by grants from JSPS KAKENHI (15H01215, 15K07931,

416 18K06627, 21K06528), The Kurata Memorial Hitachi Science and Technology

417 Foundation, Takeda Science Foundation, Daiichi Sankyo Foundation of Life Science,

418 Sagawa Foundation for Promotion of Cancer Research, Mochida Memorial Foundation

419 for Medical and Pharmaceutical Research and Foundation for Nara Institute of Science

420 and Technology.

421

Competing interests

The authors declare no competing financial interests.

References

An, J., Liu, Z., Liang, Q., Pan, Y., Li, H., Wang, R. and Jin, Y. (2017). Overexpression of Rabl3 and Cullin7 is associated with pathogenesis and poor prognosis in hepatocellular carcinoma. *Hum Pathol* **67**, 146-151.

Bhogaraju, S., Taschner, M., Morawetz, M., Basquin, C. and Lorentzen, E. (2011). Crystal structure of the intraflagellar transport complex 25/27. *EMBO J* **30**, 1907-18.

Blacque, O. E., Scheidel, N. and Kuhns, S. (2018). Rab GTPases in cilium formation and function. *Small GTPases* **9**, 76-94.

Chen, J. K., Taipale, J., Cooper, M. K. and Beachy, P. A. (2002a). Inhibition of Hedgehog signaling by direct binding of cyclopamine to Smoothened. *Genes Dev* **16**, 2743-8.

Chen, Z., Indjeian, V. B., McManus, M., Wang, L. and Dynlacht, B. D. (2002b). CP110, a cell cycle-dependent CDK substrate, regulates centrosome duplication in human cells. *Dev Cell* **3**, 339-50.

Colicelli, J. (2004). Human RAS superfamily proteins and related GTPases. *Sci STKE* **2004**, RE13.

Dateyama, I., Sugihara, Y., Chiba, S., Ota, R., Nakagawa, R., Kobayashi, T. and Itoh, H. (2019). RABL2 positively controls localization of GPCRs in mammalian primary cilia. *J Cell Sci* **132**, jcs224428.

Duan, S., Li, H., Zhang, Y., Yang, S., Chen, Y., Qiu, B., Huang, C., Wang, J., Li, J., Zhu, X. et al. (2021). Rabl2 GTP hydrolysis licenses BBSome-mediated export to fine-tune ciliary signaling. *EMBO J* **40**, e105499.

Eguether, T. and Hahne, M. (2018). Mixed signals from the cell's antennae: primary cilia in cancer. *EMBO Rep* **19**, e46589.

Ganga, A. K., Kennedy, M. C., Oguchi, M. E., Gray, S., Oliver, K. E., Knight, T. A., De La Cruz, E. M., Homma, Y., Fukuda, M. and Breslow, D. K. (2021). Rab34 GTPase mediates ciliary membrane formation in the intracellular ciliogenesis pathway. *Curr Biol* **31**, 2895-2905.e7.

Ge, T., Wu, H. C., Zhou, Y. Y., Shen, S. M., Zhu, L. G. and You, G. X. (2019). MiR-296-3p may affect the proliferation and migration of non-small cell lung cancer cells via regulating RABL3. *Eur Rev Med Pharmacol Sci* **23**, 5823-5830.

Homma, Y., Hiragi, S. and Fukuda, M. (2021). Rab family of small GTPases: an updated view on their regulation and functions. *FEBS J* **288**, 36-55.

Insinna, C., Lu, Q., Teixeira, I., Harned, A., Semler, E. M., Stauffer, J., Magidson, V., Tiwari, A., Kenworthy, A. K., Narayan, K. et al. (2019). Investigation of F-BAR domain PACSIN proteins uncovers membrane tubulation function in cilia assembly and transport. *Nat Commun* **10**, 428.

Ishikawa, H. and Marshall, W. F. (2011). Ciliogenesis: building the cell's antenna. *Nat Rev Mol Cell Biol* **12**, 222-34.

Kanie, T., Abbott, K. L., Mooney, N. A., Plowey, E. D., Demeter, J. and Jackson, P. K. (2017). The CEP19-RABL2 GTPase Complex Binds IFT-B to Initiate Intraflagellar Transport at the Ciliary Base. *Dev Cell* **42**, 22-36.e12.

Katoh, Y., Nozaki, S., Hartanto, D., Miyano, R. and Nakayama, K. (2015). Architectures of multisubunit complexes revealed by a visible immunoprecipitation assay using fluorescent fusion proteins. *J Cell Sci* **128**, 2351-62.

Knödler, A., Feng, S., Zhang, J., Zhang, X., Das, A., Peränen, J. and Guo, W. (2010). Coordination of Rab8 and Rab11 in primary ciliogenesis. *Proc Natl Acad Sci U S A* **107**, 6346-51.

Kobayashi, T. and Dynlacht, B. D. (2011). Regulating the transition from centriole to basal body. *J Cell Biol* **193**, 435-44.

Kobayashi, T., Kim, S., Lin, Y. C., Inoue, T. and Dynlacht, B. D. (2014). The CP110-interacting proteins Talpid3 and Cep290 play overlapping and distinct roles in cilia assembly. *J Cell Biol* **204**, 215-29.

Kobayashi, T., Nakazono, K., Tokuda, M., Mashima, Y., Dynlacht, B. D. and Itoh, H. (2017). HDAC2 promotes loss of primary cilia in pancreatic ductal adenocarcinoma. *EMBO Rep* **18**, 334-343.

Kobayashi, T., Tanaka, K., Mashima, Y., Shoda, A., Tokuda, M. and Itoh, H. (2020). CEP164 Deficiency Causes Hyperproliferation of Pancreatic Cancer Cells. *Front Cell Dev Biol* **8**, 587691.

Kobayashi, T., Tsang, W. Y., Li, J., Lane, W. and Dynlacht, B. D. (2011). Centriolar kinesin Kif24 interacts with CP110 to remodel microtubules and regulate ciliogenesis. *Cell* **145**, 914-25.

Li, Q., Wang, L., Zeng, L., Zhang, Y., Li, K., Jin, P. and Su, B. (2010). Evaluation of the novel gene Rabl3 in the regulation of proliferation and motility in human cancer cells. *Oncol Rep* **24**, 433-40.

Liew, G. M., Ye, F., Nager, A. R., Murphy, J. P., Lee, J. S., Aguiar, M., Breslow, D. K., Gygi, S. P. and Nachury, M. V. (2014). The intraflagellar transport protein IFT27 promotes BBSome exit from cilia through the GTPase ARL6/BBS3. *Dev Cell* **31**, 265-278.

Liu, H., Kiseleva, A. A. and Golemis, E. A. (2018). Ciliary signalling in cancer. *Nat Rev Cancer* **18**, 511-524.

Liu, Q., Tan, G., Levenkova, N., Li, T., Pugh, E. N., Rux, J. J., Speicher, D. W. and Pierce, E. A. (2007). The proteome of the mouse photoreceptor sensory cilium complex. *Mol Cell Proteomics* **6**, 1299-317.

Lu, Q., Insinna, C., Ott, C., Stauffer, J., Pintado, P. A., Rahajeng, J., Baxa, U., Walia, V., Cuenca, A., Hwang, Y. S. et al. (2015). Early steps in primary cilium assembly require EHD1/EHD3-dependent ciliary vesicle formation. *Nat Cell Biol* **17**, 228-240.

Ma, Y., Ren, Y., Wen, H. and Cui, C. (2021). circCOL1A1 Promotes the Progression of Gastric Cancer Cells through Sponging miR-145 to Enhance RABL3 Expression. *J Immunol Res* **2021**, 6724854.

Nakayama, K. and Katoh, Y. (2018). Ciliary protein trafficking mediated by IFT and BBSome complexes with the aid of kinesin-2 and dynein-2 motors. *J Biochem* **163**, 155-164.

Nishijima, Y., Hagiya, Y., Kubo, T., Takei, R., Katoh, Y. and Nakayama, K. (2017). RABL2 interacts with the intraflagellar transport-B complex and CEP19 and participates in ciliary assembly. *Mol Biol Cell* **28**, 1652-1666.

Nissim, S., Leshchiner, I., Mancias, J. D., Greenblatt, M. B., Maertens, O., Cassa, C. A., Rosenfeld, J. A., Cox, A. G., Hedgepeth, J., Wucherpfennig, J. I. et al. (2019). Mutations in RABL3 alter KRAS prenylation and are associated with hereditary pancreatic cancer. *Nat Genet* **51**, 1308-1314.

Pan, Y., Liu, Z., Feng, Z., Hui, D., Huang, X., Tong, D. and Jin, Y. (2017). The overexpression of Rabl3 is associated with pathogenesis and clinicopathologic variables in hepatocellular carcinoma. *Tumour Biol* **39**, 1010428317696230.

Ran, F. A., Hsu, P. D., Wright, J., Agarwala, V., Scott, D. A. and Zhang, F. (2013). Genome engineering using the CRISPR-Cas9 system. *Nat Protoc* **8**, 2281-2308.

Reiter, J. F. and Leroux, M. R. (2017). Genes and molecular pathways underpinning ciliopathies. *Nat Rev Mol Cell Biol* **18**, 533-547.

Shakya, S. and Westlake, C. J. (2021). Recent advances in understanding assembly of the primary cilium membrane. *Fac Rev* **10**, 16.

SOROKIN, S. (1962). Centrioles and the formation of rudimentary cilia by fibroblasts and smooth muscle cells. *J Cell Biol* **15**, 363-77.

Spektor, A., Tsang, W. Y., Khoo, D. and Dynlacht, B. D. (2007). Cep97 and CP110 suppress a cilia assembly program. *Cell* **130**, 678-90.

Stuck, M. W., Chong, W. M., Liao, J. C. and Pazour, G. J. (2021). Rab34 is necessary for early stages of intracellular ciliogenesis. *Curr Biol* **31**, 2887-2894.e4.

Sánchez, I. and Dynlacht, B. D. (2016). Cilium assembly and disassembly. *Nat Cell Biol* **18**, 711-7.

Usman, M., Ilyas, A., Hashim, Z. and Zarina, S. (2020). Identification of GIMAP7 and Rabl3 as Putative Biomarkers for Oral Squamous Cell Carcinoma Through Comparative Proteomic Approach. *Pathol Oncol Res* **26**, 1817-1822.

Walia, V., Cuenca, A., Vetter, M., Insinna, C., Perera, S., Lu, Q., Ritt, D. A., Semler, E., Specht, S., Stauffer, J. et al. (2019). Akt Regulates a Rab11-Effector Switch Required for Ciliogenesis. *Dev Cell* **50**, 229-246.e7.

Westlake, C. J., Baye, L. M., Nachury, M. V., Wright, K. J., Ervin, K. E., Phu, L., Chalouni, C., Beck, J. S., Kirkpatrick, D. S., Slusarski, D. C. et al. (2011). Primary cilia membrane assembly is initiated by Rab11 and transport protein particle II (TRAPPII) complex-dependent trafficking of Rabin8 to the centrosome. *Proc Natl Acad Sci U S A* **108**, 2759-64.

Wu, C. T., Chen, H. Y. and Tang, T. K. (2018). Myosin-Va is required for preciliary vesicle transportation to the mother centriole during ciliogenesis. *Nat Cell Biol* **20**, 175-185.

Xu, Z., Li, H., Lin, C., Zeng, B., Chen, Y. and Luo, Y. (2021). Knockdown of RABL3 suppresses the proliferation and invasion of oral squamous cell carcinoma through inactivating the FAK/AKT pathway. *J Bioenerg Biomembr* **53**, 203-211.

Xue, B., Liu, Y. X., Dong, B., Wingfield, J. L., Wu, M., Sun, J., Lechtreck, K. F. and Fan, Z. C. (2020). Intraflagellar transport protein RABL5/IFT22 recruits the BBSome to the basal body through the GTPase ARL6/BBS3. *Proc Natl Acad Sci U S A* **117**, 2496-2505.

Zhang, W., Sun, J. and Luo, J. (2016). High Expression of Rab-like 3 (Rabl3) is Associated with Poor Survival of Patients with Non-Small Cell Lung Cancer via Repression of MAPK8/9/10-Mediated Autophagy. *Med Sci Monit* **22**, 1582-8.

Zhong, X., Su, L., Yang, Y., Nair-Gill, E., Tang, M., Anderton, P., Li, X., Wang, J., Zhan, X., Tomchick, D. R. et al. (2020). Genetic and structural studies of RABL3 reveal an essential role in lymphoid development and function. *Proc Natl Acad Sci U S A* **117**, 8563-8572.

Figure Legends

Figure 1

RABL3 depletion impairs primary cilia formation in RPE1 cells

(A) Indicated cells were cultured for 48 hrs. Cell extracts were immunoblotted with an anti-RABL3 antibody. β-Actin was used as a loading control. **(B, C)** Indicated cells were cultured in serum-starved medium for 24 hrs and immunostained with anti-glutamylated tubulin (GT335, red) and anti-Arl13b (green) antibodies. (B) DNA was stained with Hoechst (blue). Scale bar, 5 μm. (C) The percentage of cells with primary cilia was determined. Average of three independent experiments is shown. >250 cells were scored for each experiment. **(D, E)** Indicated cells transfected with plasmids expressing EGFP and mock, Flag-hRABL3/WT, or S20N were cultured in serum-starved medium for 24 hrs and immunostained with an anti-glutamylated tubulin antibody (red). (D) DNA was stained with Hoechst (blue). Scale bar, 5 μm. (E) The percentage of GFP-positive cells with primary cilia was determined. Average of three independent experiments is shown. >100 cells were scored for each experiment. **(F, G)** RPE1 cells transfected with indicated siRNA were cultured in serum-starved medium for 48 hrs. (F) Cell extracts were immunoblotted with indicated antibodies. β-Actin was used as a loading control. (G) Cells were immunostained with an anti-glutamylated tubulin antibody. The percentage of cells with primary cilia was determined. Average of three independent experiments is shown. >250 cells were scored for each experiment. **(C, E, G)** Error bars represent SD. *: $p < 0.05$, **: $p < 0.01$ compared with RPE1 (A), Mock (E), or siLuc (F).

Figure 2

RAB11 interacts with and stabilizes RABL3

(A, B) Flag-RABL3/WT (W) or S20N (S) and GFP-RAB11A/WT (W), Q70L (Q) or S25N (S) were expressed in HEK293T cells. Lysates were immunoprecipitated with (A) anti-Flag or (B) anti-GFP (GFP-nanobody) antibodies. The resulting immunoprecipitates were western blotted with indicated antibodies. **(C)** Purified recombinant proteins visualized by Coomassie stain. **(D)** Recombinant RABL3, GST-RAB11 and GST proteins were subjected to *in vitro* binding assay in the presence of indicated additives. The resulting precipitates were immunoblotted with indicated antibodies. **(E)** Recombinant RABL3, GST-RAB11 and GST were subjected to Turbidity assay. The optimal density at 350 nm of the protein solution was determined every 3 mins. Average of three independent experiments is shown.

Error bars represent SD. *: $p < 0.05$, **: $p < 0.01$ compared with GST + RABL3.

Figure 3

RABL3 accumulates around centrosomes during early ciliogenesis

(A, B) Indicated cells were cultured in serum-fed medium for 48 hrs (left) or serum-starved medium for 6 hrs (right) and immunostained with anti-glutamylated tubulin (green) and anti-RABL3 (red) antibodies. (A) DNA was stained with Hoechst (blue). Scale bar, 10 μm. (B) The quantified fluorescence intensity of RABL3 within ~3 μm diameter circle around centrosome is shown. n = 25 (FBS +), 28 (Starvation 6 h). **(C)** RPE1 cells were cultured in serum-starved medium for 6 hrs and immunostained with anti-CEP164 (green), anti-RABL3 (red), and anti-RAB11 (blue) antibodies. Scale bar,

609 2.5 μm. **(D, E)** RPE1 cells were cultured in serum-starved medium for 6 hrs and
610 immunostained with anti-RABL3 (red) and (D) anti-RAB11 (green) or (E) anti-GM130
611 (green) antibodies. DNA was stained with Hoechst (blue). Scale bar, 10 μm. **(E)** RPE1
612 cells transfected with plasmids expressing Myc-hRABL3/WT (left) or S20N (right) were
613 cultured in serum-starved medium for 6 hrs and immunostained with anti-glutamylated
614 tubulin (green) and anti-Myc (red) antibodies. Two representative images are shown.
615 DNA was stained with Hoechst (blue). Scale bar, 5 μm.
616 **(B)** Error bars represent SD. **: $p < 0.01$ compared with FBS +.

617 **Figure 4**

618 **RABL3 is required for early ciliogenesis**

619 **(A, B)** RPE1 cells transiently transfected with indicated siRNA were cultured in
620 serum-starved medium for 48 hrs. Cells were immunostained with anti-glutamylated
621 tubulin (green), anti-centrin (green), and anti-CP110 (red) antibodies. (A) DNA was
622 stained with Hoechst (blue). Scale bar, 5 μm. (B) The percentage of cells with two
623 CP110 dots at non-ciliated centrosome was determined. Average of three to four
624 independent experiments is shown. >100 cells were scored for each experiment. **(C, D)**
625 GFP-Rabin8-RPE1 cells transiently transfected with indicated siRNA were cultured in
626 serum-starved medium for 1 hr. Cells were immunostained with anti-glutamylated
627 tubulin (red) and anti-centrin (red) antibodies. (C) DNA was stained with Hoechst (blue).
628 Scale bar, 2.5 μm. (D) The quantified fluorescence intensity of GFP-Rabin8 within ~3
629 μm diameter circle around non-ciliated centrosome is shown. n = 37 (siLuc), 32
630 (siRABL3#1), 23 (siRABL3#2), 24 (siRAB11A+B).

631 **(B, D)** Error bars represent SD. **: $p < 0.01$ compared with siLuc (B, D).

632 **Figure 5**

633 **RABL3 positively controls CV formation like RAB11**

634 **(A, B)** GFP-SMO-RPE1 cells transiently transfected with indicated siRNA were
635 cultured in serum-starved medium for 48 hrs. Cells were immunostained as described in
636 Figure 4C. (A) DNA was stained with Hoechst (blue). Scale bar, 5 μm. (B) The
637 percentage of cells with SMO-negative centrosome (cilia - & SMO -), SMO-positive
638 centrosome (cilia - & SMO +), or SMO-positive cilia (cilia + & SMO +) was
639 determined. Average of three independent experiments is shown. >100 cells were scored
640 for each experiment. **(C, D)** Indicated cells were cultured in serum-starved medium for
641 3 (T3) or 6 (T6) hrs and immunostained with anti-glutamylated tubulin (green) and
642 anti-Myo-Va (red) antibodies. (C) Representative Myo-Va-positive or -negative
643 centrosome in RPE1 cells. DNA was stained with Hoechst (blue). Scale bar, 2.5 μm. (D)
644 The percentage of cells with Myo-Va-dot at non-ciliated centrosome was determined.
645 Average of three independent experiments is shown. >100 cells were scored for each
646 experiment. **(E)** RPE1 cells transiently transfected with indicated siRNA were cultured
647 and immunostained as described in Figure 5C. The percentage of cells with Myo-Va-dot
648 at non-ciliated centrosome was determined. Average of three independent experiments
649 is shown. >100 cells were scored for each experiment. **(F)** RPE1 cells transfected with
650 plasmids expressing EGFP and indicated proteins were cultured and immunostained as
651 described in Figure 5C. The percentage of cells with Myo-Va-dot at non-ciliated
652 centrosome was determined. Average of three to four independent experiments is shown.

653 >100 cells were scored for each experiment. **(G)** RPE1 or Rabl3-1 cells transfected with
654 plasmids expressing EGFP and RAB11A/ Q70L were cultured and immunostained as
655 described in Figure 5C. The percentage of cells with Myo-Va-dot at non-ciliated
656 centrosome was determined. Average of four independent experiments is shown. >100
657 cells were scored for each experiment.
658 **(B-G)** Error bars represent SD. *: $p < 0.05$, **: $p < 0.01$ compared with RPE1 (D),
659 siLuc (E), Mock (F), or RPE1 + RAB11A/QL (G). #: $p < 0.05$, ##: $p < 0.01$ compared
660 with siRAB8A + B (B).
661

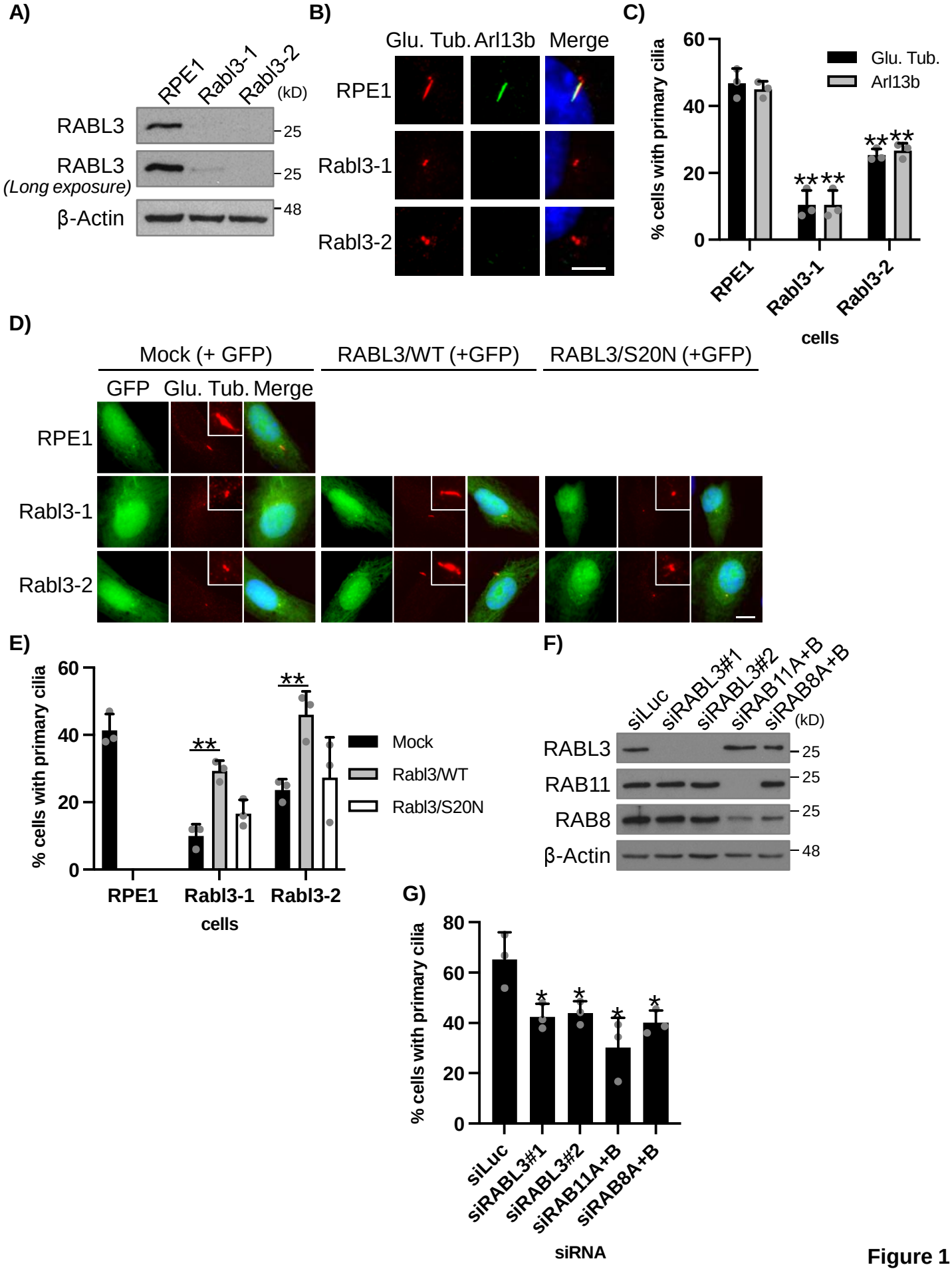

Figure 1

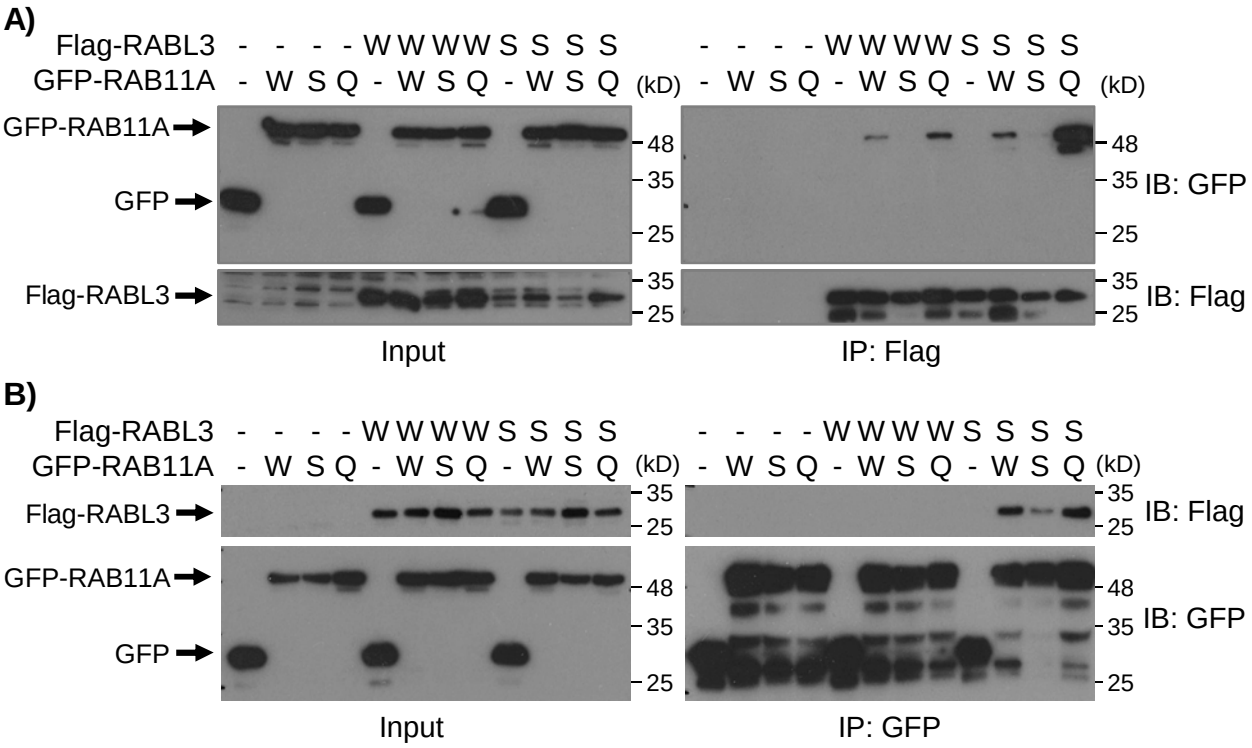

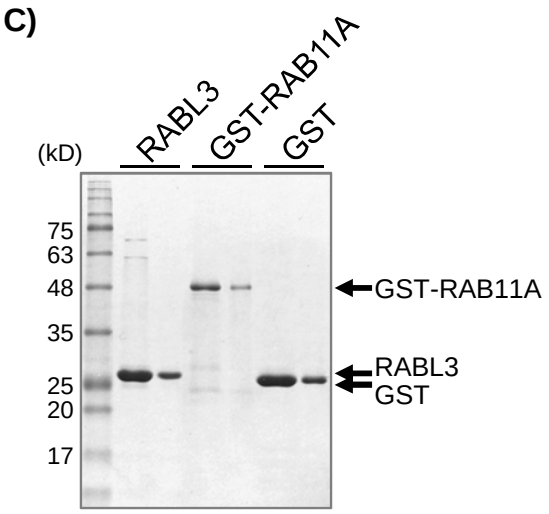

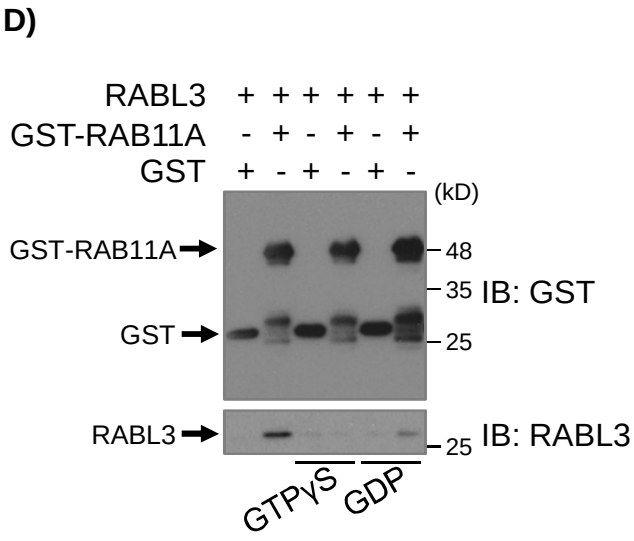

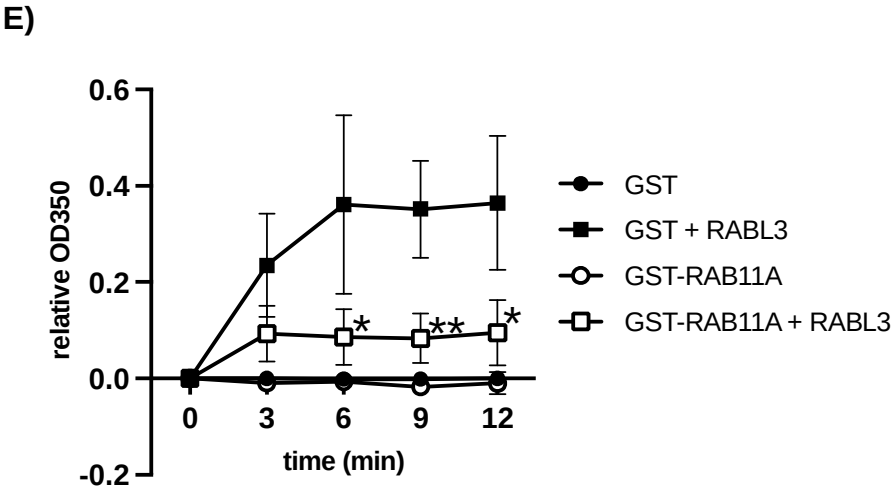

Figure 2

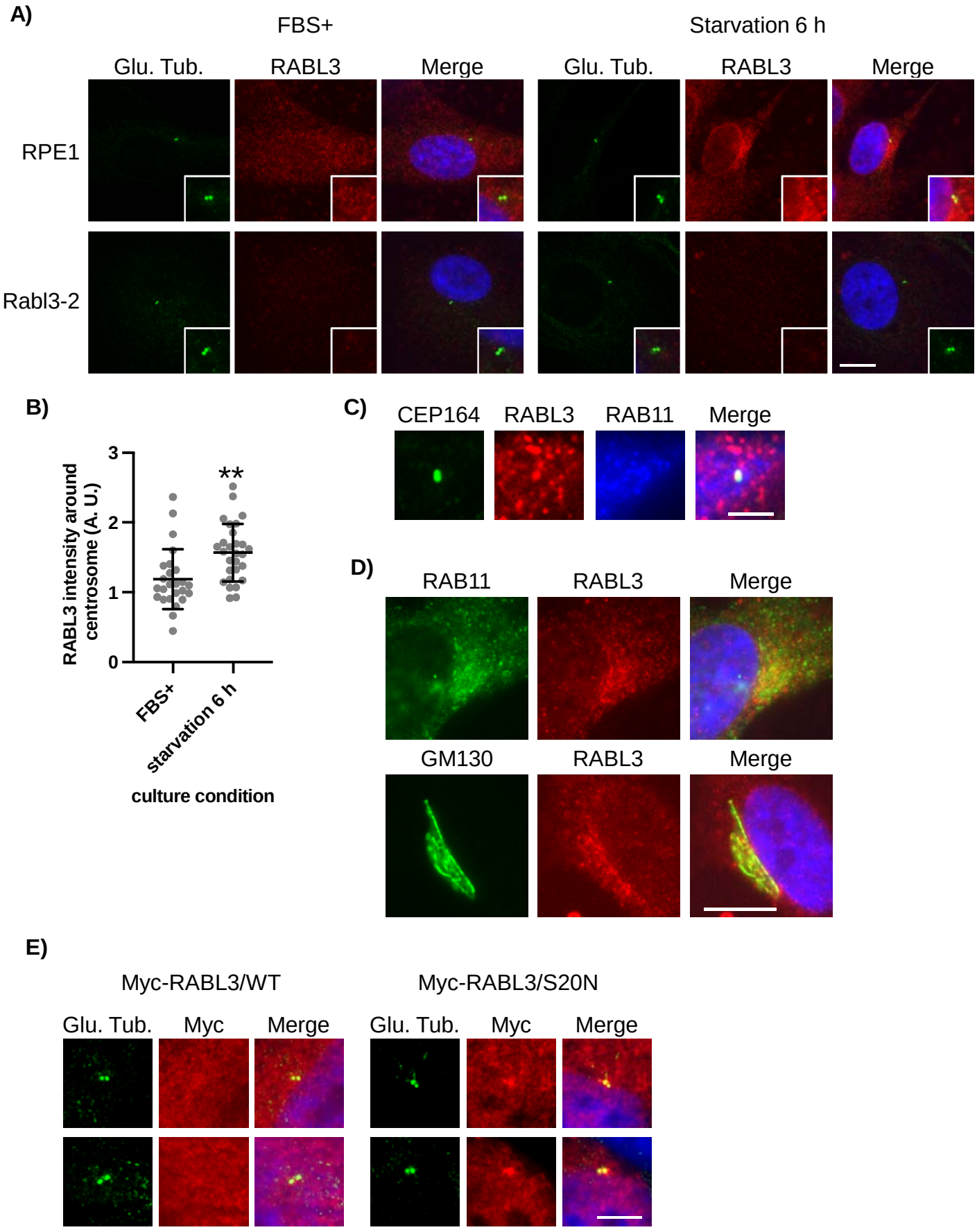

Figure 3

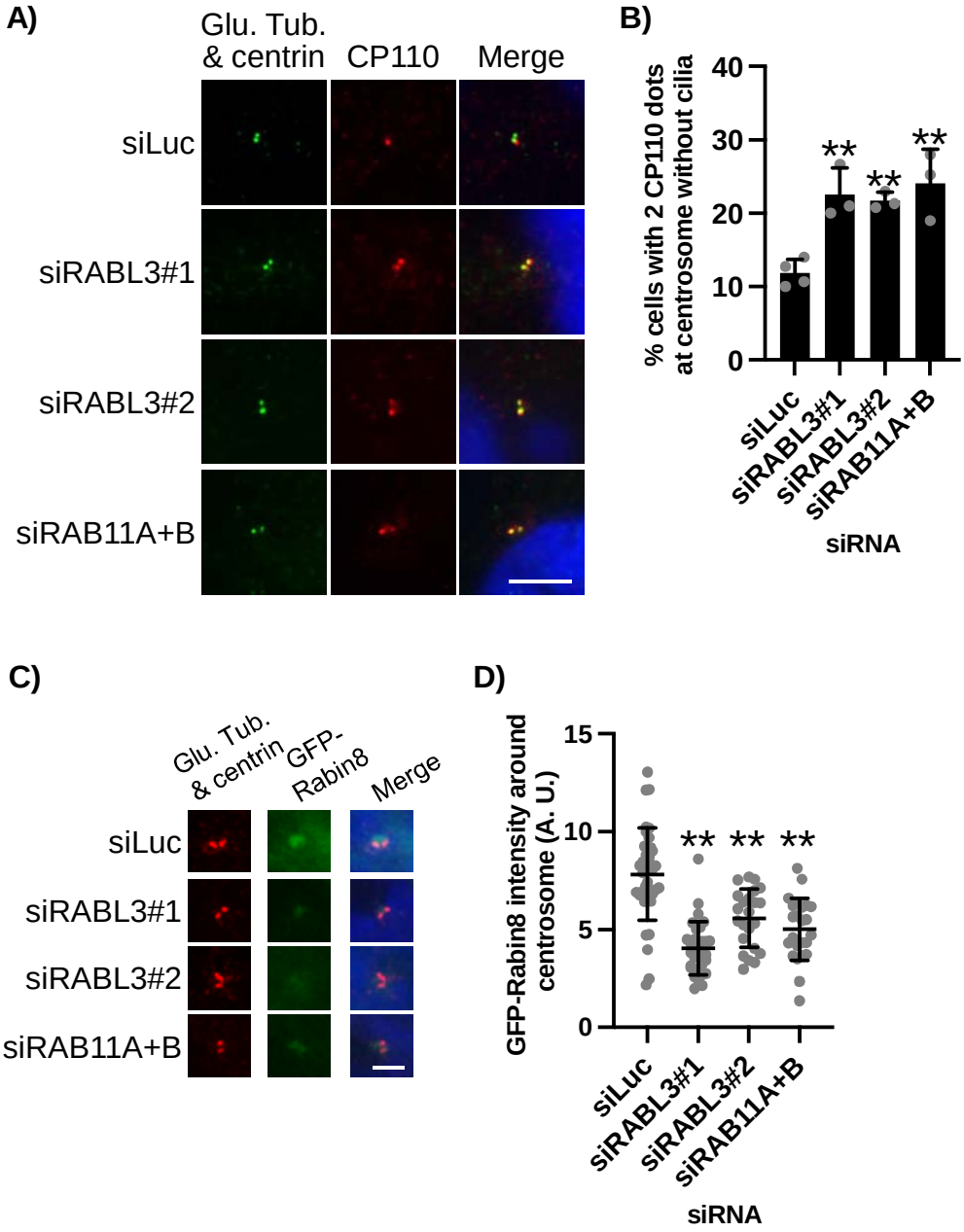

Figure 4

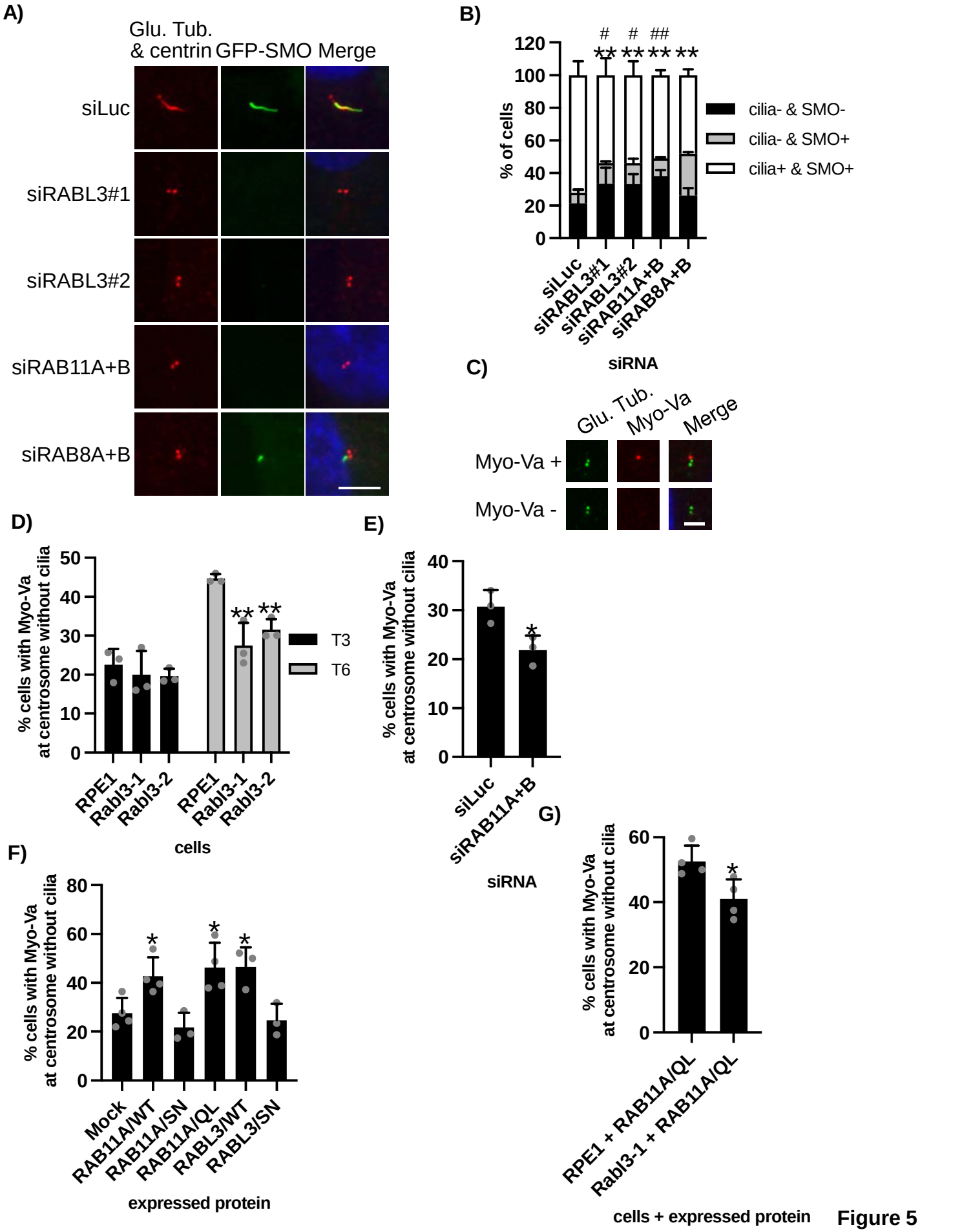

Figure 5